Journal of Electronic Research and Application, 2025, Volume 9, Issue 3
http://ojs.bbwpublisher.com/index.php/JERA
ISSN Online: 2208-3510
ISSN Print: 2208-3502

Retinal Vessel Segmentation based on Improved PCNN and Gray Wolf Optimization Algorithm

Xingfu Ou[1], Miao Zhang[2], Wenfeng Chen[1]*

[1]Institute of Intelligent Manufacturing Foshan Polytechnic, Foshan 528137, Guangdong, China
[2]College of Automation Guangdong University of Technology, Guangzhou 510006, Guangdong, China

**Author to whom correspondence should be addressed.*

Abstract: Since the problems of branch loss and fracture in retinal blood vessel segmentation algorithms, an image segmentation method is proposed based on improved pulse coupled neural network (PCNN) and gray wolf optimization algorithm (GWO). Simplifying the neuron input domain and neuron connection domain of the PCNN network, increasing the gradient information factor in the internal activity items, reducing the model parameters, enhancing the pulse issuing ability, and the optimal parameters of the network are automatically obtained based on multiple feature evaluation criteria and the GWO algorithm. The test in the public data set drive shows that the sensitivity, accuracy, precision, and specificity of the algorithm are 0.799549, 0.962789, 0.889163, and 0.986552, respectively. The accuracy and specificity are better than the classical segmentation algorithm. It solved the influence of low illumination, optic disc highlight, and foveal shadow on vascular segmentation, and showed excellent performance of vessel connectivity and terminal sensitivity.

Keywords: Retinal blood vessel; Image segmentation; PCNN; GWO; Parameter adaptation; Multi-feature evaluation criteria

Online publication: 5 June, 2025

1. Introduction

As a "window" to human blood vessels, retinal blood vessels at the fundus of the eyeball provide important reference information for the diagnosis of diseases such as hemangioma, cataract, and diabetes. Usually, clinical personnel manually analyze the shape, color, curvature, and position information of blood vessels in fundus retinal images to analyze and diagnose the above diseases. However, due to the complex structure of fundus retinal blood vessels and the difficulty of observation, the detection effect depends on the clinical experience of medical personnel, and the manual method is time-consuming and labor-intensive, and cannot meet the requirements of real-time automatic analysis.

At present, many domestic and foreign researchers have proposed applying digital image processing technology to the field of human fundus retinal blood vessel recognition, and have proposed different retinal blood vessel feature intelligent extraction technologies based on various algorithm principles. For example, Wang used particle swarm optimization and maximum entropy method of grayscale-gradient co-occurrence matrix for threshold segmentation [1]. Meng *et al.* designed a method for preprocessing and edge detection of fundus retinal blood vessels using the Frangi filter and a morphological algorithm [2]. Luiz *et al.* used spatial correlation, probability statistical information, and curvature analysis to improve the accuracy of blood vessel segmentation [3]. Li *et al.* proposed to construct 4D feature vectors based on fused phase features and use a support vector machine (SVM) for blood vessel pixel classification [4]. Cheng and Americo proposed a new U-Net network structure for retinal vascular segmentation [5,6], which solved the problem of different widths and directions of retinal vascular structures. However, because the fundus vascular network is small and not prominent, and the difference from the background is not obvious, the grayscale feature-based algorithm still has problems, such as loss of vascular branches and breakage, and the segmentation accuracy based on the deep learning algorithm is affected by the manually labeled training dataset.

This paper proposes an improved PCNN network model based on GWO automatic parameter setting for fundus retinal vascular image segmentation. (1) An improved PCNN model is proposed to solve the problems of the traditional PCNN network model being too complex and inefficient, and to make the fundus retinal vascular image segmentation more precise and with higher processing resolution. (2) A method for obtaining PCNN model parameters based on GWO is proposed to solve the problem of adaptive optimization of model parameters. (3) An image segmentation evaluation standard based on multiple features is designed to solve the convergence and image segmentation accuracy of GWO.

2. Retinal vessel segmentation algorithm

Figure 1 shows the segmentation algorithm framework. The fundus color image is split into channels, and the G channel grayscale image is extracted and enhanced. Gaussian filtering and the Laplace operator are applied in the PCNN feedback domain for image smoothing. The GWO algorithm optimizes PCNN parameters by maximizing a fitness function based on minimum cross-entropy, shape metrics, and regional consistency. The PCNN generates an ignition map, which is binarized with a fixed threshold. Finally, the eyeball contour edges are masked out to produce the final vascular segmentation.

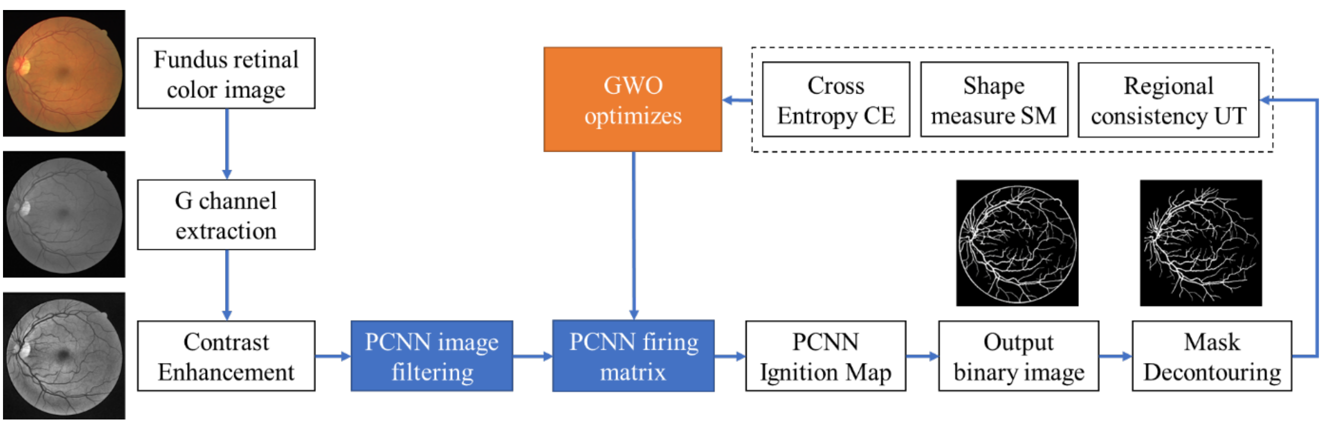

Figure 1. Flow chart of the proposed algorithm

3. Improved PCNN model

The PCNN model is derived from the mathematical abstraction of biological neurons. Its structure is similar to that of biological neurons, including input domain, connection domain, and pulse generation domain. The discrete mathematical iterative equation can be expressed as Equations (1) to (5).

$$F_{ij}[n] = e^{-\alpha_F} F_{ij}[n-1] + S_{ij} + V_F \sum_{kj} \boldsymbol{M}_{ij,kl} Y_{kl}[n-1] \tag{1}$$

$$L_{ij}[n] = e^{-\alpha_L} L_{ij}[n-1] + V_L \sum_{kj} \boldsymbol{W}_{ij,kl} Y_{kl}[n-1] \tag{2}$$

$$U_{ij}[n] = F_{ij}[n](1 + \gamma L_{ij}[n]) \tag{3}$$

$$Y_{ij}[n] = \begin{cases} 1, & U_{ij}[n] > E_{ij}[n] \\ 0, & U_{ij}[n] \le E_{ij}[n] \end{cases} \tag{4}$$

$$E_{ij}[n] = e^{-\alpha_E} E_{ij}[n-1] + V_E Y_{ij}[n]) \tag{5}$$

(i,j) and (k,l) denote the target neuron and its neighboring neuron labels, and n is the number of iterations. S_{ij} represents the pixel grayscale value. The neuron's feedback input F_{ij} and connection input L_{ij} link to neighboring neurons through coefficient matrices $\boldsymbol{M}$ and $\boldsymbol{W}$, decaying from amplitudes V_F and V_L with decay parameters α_F and α_L. These inputs are modulated by connection strength γ to form the internal activity U_{ij}, which is compared to a dynamic threshold E_{ij} defined by amplitude V_E and decay constant α_E. The neuron fires based on this comparison, outputting pulse Y_{ij}. Neurons with similar states fire synchronously to segment different image regions sequentially.

However, the traditional PCNN model is overly complex, with many parameters and fixed connection domains, making it unsuitable for adaptive image segmentation. Thus, optimizing the network structure to enhance neuron firing, reduce parameters, and improve segmentation performance is necessary.

3.1. Model structure optimization

Based on the traditional PCNN model, the optimized PCNN model is shown in **Figure 2**.

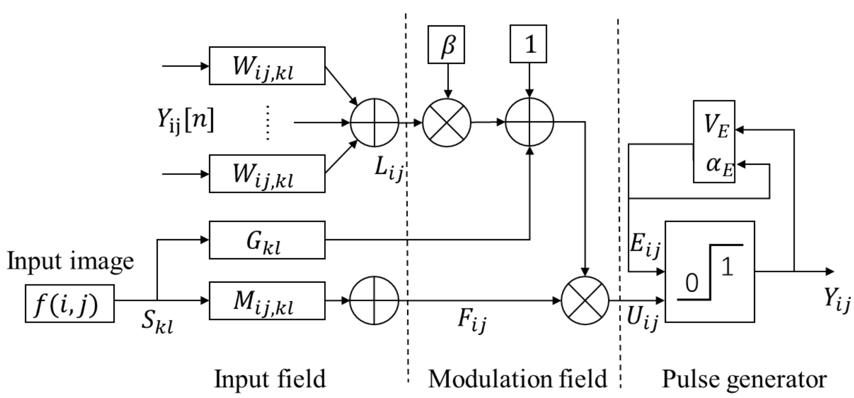

Figure 2. Improved PCNN model structure

In the model, the leaky integral attenuation mechanism is firstly cancelled in the input domain, and the feedback input item F_{ij} is the coupling of the grayscale value S_{kl} of the pixel point in the image area and the connection coefficient matrix $\boldsymbol{M}_{ij,kl}$ as the external signal of the neuron, to suppress the interference of image spatial noise and enhance the image edge information. The mathematical expression is as follows:

$$F_{ij}[n] = \sum_{kj} \boldsymbol{M}_{ij,kl} S_{kl} \tag{6}$$

L_{ij} is the pulse output of the last iteration of the neighborhood neuron of the target pixel in the image, coupled with the connection coefficient matrix $\boldsymbol{W}_{ij,kl}$, ignoring the attenuation mechanism of the connection input. The mathematical expression is as follows:

$$L_{ij}[n] = \sum_{kj} \boldsymbol{W}_{ij,kl} Y_{kl}[n-1] \tag{7}$$

In the neuron internal activity term U_{ij} in formula (3), the strength of the mutual coupling between the current pixel and the neighboring pixels is adjusted, the edge gradient information of the local detail features of the image is integrated, and the edge features of the image target segmentation results are enhanced. The expression is as follows:

$$U_{ij}[n] = F_{ij}[n](1 + G_{ij} + \gamma L_{ij}[n]) \tag{8}$$

The dynamic threshold and pulse output mechanism of the model are retained, as shown in equations (4) and (5).

3.2. Connection coefficient matrix optimization

Usually, medical images will generate image noise due to various factors during the acquisition, conversion, and processing. To effectively suppress the noise, a Gaussian filter function is used in the feedback input domain to perform linear smoothing on the image to reduce the influence of Gaussian noise, as shown in formula (9).

$$\boldsymbol{M}_G = \boldsymbol{C}_g \bullet \frac{1}{2\pi\sigma_1\sigma_2} \exp[-\frac{1}{2}(\frac{\|k-i\|^2}{\sigma_1^{\ 2}} - \frac{\|j-l\|^2}{\sigma_1^{\ 2}})] \tag{9}$$

To address the edge-blurring effect of Gaussian filtering, this paper integrates the Gaussian filter with the Laplace energy function to construct the feedback input connection coefficient matrix of the PCNN model. The Laplace energy function preserves target clarity and edge contrast. This fusion enables both edge protection and spatial noise suppression. The mathematical expressions are shown in formulas (10) and (11).

$$\boldsymbol{M}_P = C_P(\frac{\partial^2 f}{\partial i^2} + \frac{\partial^2 f}{\partial j^2}) = C_P(\sum S_{kl} - 4S_{ij}) \tag{10}$$

$$\boldsymbol{M}_{ij,kl} = \begin{cases} \boldsymbol{M}_G, & Y_{ij}[n-1] = 0 \quad or \quad Y_{kl}[n-1] = 0 \\ \boldsymbol{M}_P, & otherwise \end{cases} \tag{11}$$

Here, C_g and C_p are normalization coefficients, and σ_1, σ_2 are Gaussian scaling factors. S_{ij} and S_{kl} represent the grayscale values of the target and neighboring pixels, respectively. Due to significant grayscale differences between spatial noise and its neighbors, the PCNN's neighborhood similarity-based ignition function is used to detect Gaussian noise. If detected, the Gaussian filter constructs the feedback input connection matrix; otherwise, the Laplace energy function is used.

The connection matrix $\boldsymbol{W}_{ij,kl}$ adjusts the ignition state of neighboring neurons from the previous iteration, traditionally computed using the Euclidean distance between the target and neighboring pixels, as expressed below.

$$\boldsymbol{W}_{ij,kl}=\frac{1}{(i-k)^2+(j-l)^2} \tag{12}$$

Considering that neuron coupling strength depends on spatial distance, previous firing states, and grayscale values, the connection coefficient matrix $\boldsymbol{W}_{ij,kl}$ is defined as follows:

$$\boldsymbol{W}_{ij,kl}=\frac{k_1}{e^{k_2(d+1)}+k_3} \tag{13}$$

Where d is the distance from the center pixel to the neighborhood boundary pixel, k_1, k_2, k_3 are fixed constants.

3.3. Optimization of coupled connection domain

In the traditional PCNN model, the feedback input F_{ij} receives pixel grayscale values, and the connection input L_{ij} receives signals from neighboring neurons. Their coupling generates the internal activity, indicating the correlation between a pixel and its neighbors, enabling synchronized firing of similar pixels. However, this ignores the impact of edge features on neuron firing. To address this, this paper incorporates image gradient information into the internal activity to enhance edge feature response, as shown in equations (14)–(16).

$$G_{ij}=\sqrt{{G_{ij,h}}^2+{G_{ij,v}}^2} \tag{14}$$

$$G_{ij,h}=\frac{1}{2}(S_{i+1,j}+S_{i+1,j+1}-S_{i,j}-S_{i,j+1}) \tag{15}$$

$$G_{ij,v}=\frac{1}{2}(S_{i,j+1}+S_{i+1,j+1}-S_{i,j}-S_{i+1,j}) \tag{16}$$

Wherein, $G_{ij,h}$ and $G_{ij,y}$ are the gradients of the image at the pixel (i, j) in the X-axis direction and the Y-axis direction, respectively.

4. Multi-feature image segmentation evaluation criteria

Traditional PCNN segmentation evaluation methods—such as maximum Shannon entropy, grayscale entropy, and variance ratio—focus mainly on optimal threshold calculation, offering limited insight and underutilizing PCNN's pulse coupling and neighborhood interaction capabilities. To achieve more accurate segmentation and preserve edge and contour details, this paper proposes a multi-feature evaluation function tailored to fundus retinal images. It combines cross entropy (CE), shape measure (SM), and regional consistency (UT), considering information content, edge details, and spatial distribution. The mathematical expression is as follows:

$$fitness=\frac{1}{CE}+SM+UT \tag{17}$$

Where:

$$CE(P,Q,t)=\sum_{f=0}^{t}[f\bullet h(f)\bullet\ln\frac{f}{\mu_1(t)}+\mu_1(t)\bullet h(f)\bullet\ln\frac{\mu_1(t)}{f}]+\sum_{f=t+1}^{T}[f\bullet h(f)\bullet\ln\frac{f}{\mu_2(t)}+\mu_2(t)\bullet h(f)\bullet\ln\frac{\mu_2(t)}{f}] \tag{18}$$

$$SM(t) = \frac{1}{C_0} \sum_{(x,y)\in f} sign(f(x,y) - \overline{f}_N)\Delta(x,y) sign(f(x,y),t) \tag{19}$$

$$UT = 1 - \frac{1}{C_1} \sum_i \left\{ \sum_{(x,y)\in R_i} \left[f(x,y) - \frac{1}{A_i} \sum_{(x,y)\in R_i}^{n} f(x,y) \right]^2 \right\} \tag{20}$$

Formula (20) is used as the evaluation criterion for fundus retinal blood vessel image segmentation to achieve parameter optimization of PCNN. The larger the fitness value function value, the better the blood vessel target segmentation effect.

5. PCNN parameter optimization algorithm based on GWO

The Grey Wolf Optimizer (GWO) is a swarm intelligence algorithm inspired by the social hierarchy and hunting strategies of gray wolves. It features strong global convergence and few parameters, outperforming PSO, ABC, GA, and BSO in accuracy and speed [7–10]. This paper uses GWO to optimize PCNN parameters, addressing issues like local optima and high computational cost [11].

5.1. Principle of GWO algorithm

GWO mimics gray wolves' hunting behaviors—tracking, encircling, and attacking prey. Wolves are ranked by fitness as α (best), β (second best), δ (third best), and ω (the rest). The top three guide the search, with ω wolves updating their positions based on their distance to the "prey" (optimal solution). The position update process is shown in **Figure 3** and defined by equations (21)–(22).

$$D = \left| \boldsymbol{C} \bullet \boldsymbol{X}_P(t) - \boldsymbol{X}(t) \right| \tag{21}$$

$$\boldsymbol{X}(t+1) = \boldsymbol{X}_P(t) - \boldsymbol{A} \bullet D \tag{22}$$

Where t is the number of iterations; D is the distance between the gray wolf and the prey, $\boldsymbol{A}$ and $\boldsymbol{C}$ are coefficient vectors, $\boldsymbol{X}$ and $\boldsymbol{X}_P$ are the position vectors of the gray wolf and the prey, respectively.

$$\boldsymbol{A} = 2\boldsymbol{\alpha} \bullet \boldsymbol{r}_1 - \boldsymbol{\alpha} \tag{23}$$

$$\boldsymbol{C} = 2\boldsymbol{r}_2 \tag{24}$$

$$\boldsymbol{\alpha} = 2(1 - \frac{t}{T_{max}})\boldsymbol{e} \tag{25}$$

Where α is the convergence factor, t and T_{max} represent the current number of iterations and the maximum number of iterations, respectively; r_1 and r_2 are random vectors with a modulus of 0 to 1, and e is a unit vector.

During the hunt, wolves update their positions based on the locations of the α, β, and δ wolves, iteratively approaching the prey. In each iteration, the top three solutions are assigned to α, β, and δ wolves. The position update is defined by the following equation:

$$D_\alpha(t) = \left| \boldsymbol{C}_1 \bullet \boldsymbol{X}_\alpha(t) - \boldsymbol{X}(t) \right| \tag{26}$$

$$X_1(t) = X_\alpha(t) - A_1 \cdot D_\alpha(t) \tag{27}$$

$$D_\beta(t) = \left| C_2 \cdot X_\beta(t) - X(t) \right| \tag{28}$$

$$X_2(t) = X_\beta(t) - A_2 \cdot D_\beta(t) \tag{29}$$

$$D_\delta(t) = \left| C_3 \cdot X_\delta(t) - X(t) \right| \tag{30}$$

$$X_3(t) = X_\delta(t) - A_3 \cdot D_\delta(t) \tag{41}$$

$$X(t+1) = \frac{1}{3}\left[X_1(t) + X_2(t) + X_3(t) \right] \tag{42}$$

Where: $\boldsymbol{X}_\alpha(t)$, $\boldsymbol{X}_\beta(t)$, $\boldsymbol{X}_\delta(t)$ are the positions of the α, β, and δ wolves at iteration t; $\boldsymbol{D}_\alpha(t)$, $\boldsymbol{D}_\beta(t)$, $\boldsymbol{D}_\delta(t)$ are their distances to a given wolf; $\boldsymbol{X}_1(t)$, $\boldsymbol{X}_2(t)$, $\boldsymbol{X}_3(t)$ are the approach vectors toward α, β, and δ wolves; $\boldsymbol{A}_1$, $\boldsymbol{A}_2$, $\boldsymbol{A}_3$ and $\boldsymbol{C}_1$, $\boldsymbol{C}_2$, $\boldsymbol{C}_3$ are random coefficient vectors; $\boldsymbol{X}(t+1)$ is the updated position for the ω wolf in the next iteration.

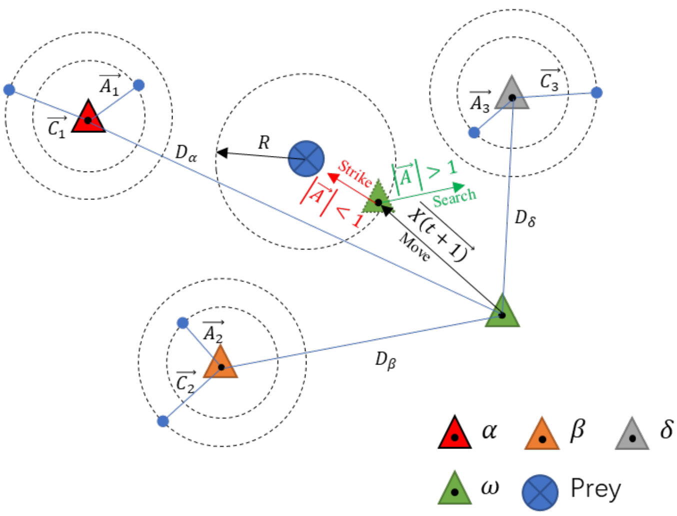

Figure 3. Location update principle of gray wolf optimization algorithm

5.2. GWO-PCNN algorithm flow

The GWO algorithm is used to adaptively optimize the time constant α_E, connection coefficient γ, and dynamic threshold amplitude V_E in the improved PCNN model for fundus vascular image segmentation, enhancing accuracy and generalization. The steps are:

Step 1: Initialize population size N, max iterations T_{max}, and GWO parameters α, r_1, and r_2 to compute vectors A and C.

Step 2: Randomly initialize wolf positions X_i using parameter bounds $R_{u,j}$, $R_{d,j}$.

Step 3: Calculate each individual's fitness using formula (20).

Step 4: Rank individuals by fitness, assign top three as X_α、 X_β, and X_δ.

Step 5: Update coefficients A_1, A_2, A_3 and C_1, C_2, C_3, compute distances $D_\alpha(t)$, $D_\beta(t)$, $D_\delta(t)$, and update position vector $X(t+1)$.

Step 6: If iteration reaches T_{max}, output X_α as the optimal solution; otherwise, repeat from Step 3.

Step 7: Use the optimal $\boldsymbol{X}_\alpha$ to construct the improved PCNN model for retinal vessel segmentation.

6. Experiment and analysis

6.1. Experimental environment

The experiments were conducted on MATLAB R2021a running on Windows 10, with an Intel Core i7-10750H CPU @2.60 GHz and 16GB RAM. The dataset used is the internationally recognized DRIVE fundus image database, consisting of 40 color retinal vascular images with corresponding expert manual segmentations. Each image has a resolution of 565 × 584.

6.2. Evaluation indicators

The algorithm's performance was assessed both subjectively by visual inspection of segmentation results and objectively using four metrics: Accuracy (Acc), Sensitivity (Sen), Specificity (Spe), and Precision (Pre). Their calculation formulas are given in equations (34)–(37):

$$Acc = (TP + TN) / (TP + TN + FP + FN) \tag{34}$$

$$Sen = TP / (TP + FN) \tag{35}$$

$$Spe = TN / (TN + FP) \tag{36}$$

$$Pri = TP / (TP + FP) \tag{37}$$

6.3. Subjective evaluation analysis

Five fundus images with varied features were randomly selected from the DRIVE dataset. The G channel images were extracted and preprocessed. PCNN parameters were initialized by the wolf pack and optimized iteratively using the GWO algorithm based on fitness values. After network activation and contouring, retinal vessel segmentation results were obtained. Some results are shown in **Figure 4**.

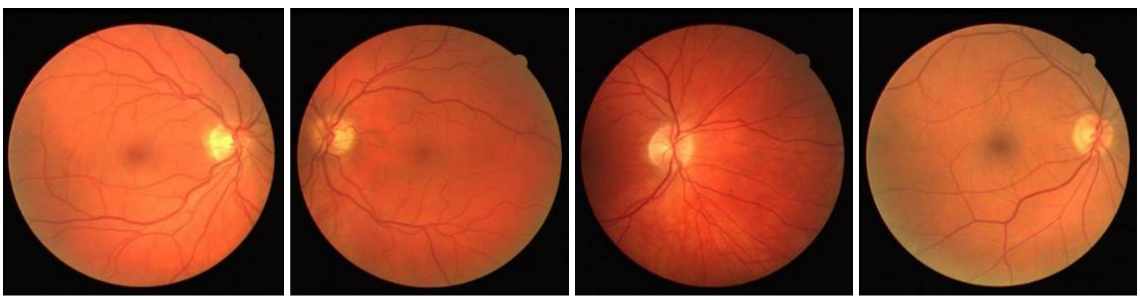

(a) Test image

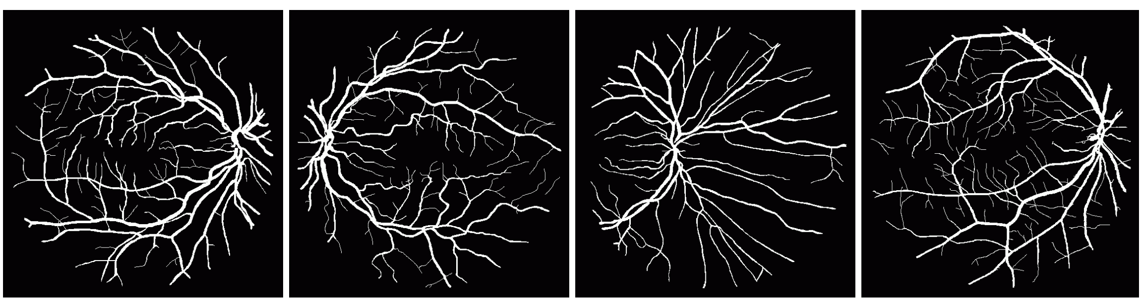

(b) Expert manual labeling results

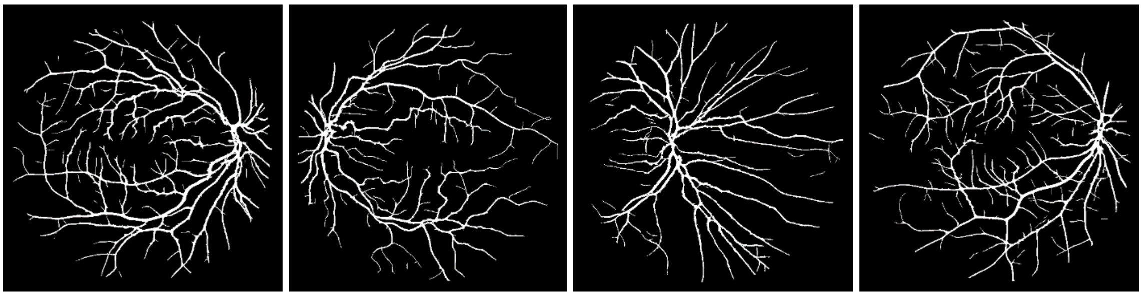

(c) Results of this algorithm

Figure 4. Segmentation results of this algorithm in drive dataset

Sub-image (a) shows test images 1 to 4 from the DRIVE fundus database, (b) shows expert manual segmentations, and (c) displays segmentation results from the proposed algorithm. The optimal GWO parameters obtained are αE = 6.5326, 7.1354, 6.3933, 7.4212, 6.1078; γ = 0.4387, 0.4854, 0.4598, 0.5837, 0.4903; VE = 212, 230, 201, 238, 242, 232. Compared to expert results, the algorithm segments thick vessels near the optic disc clearly, preserves bifurcations, intersections, parallel vessels, and most fine vessel terminals.

Figure 5 shows the parameter optimization curves for test images 1 to 4. The algorithm fluctuates slightly early on but converges near the optimal solution within 25 iterations. Randomness causes minor variations per image, but overall convergence is fast and optimization is robust.

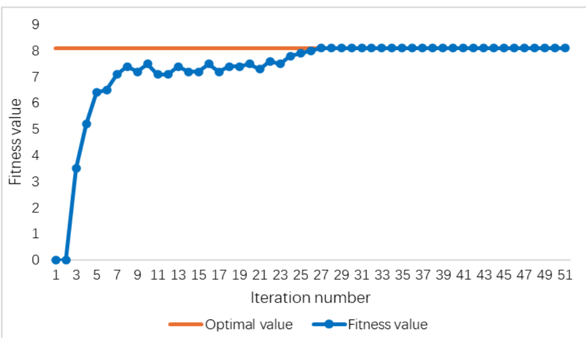

(a) Test image1

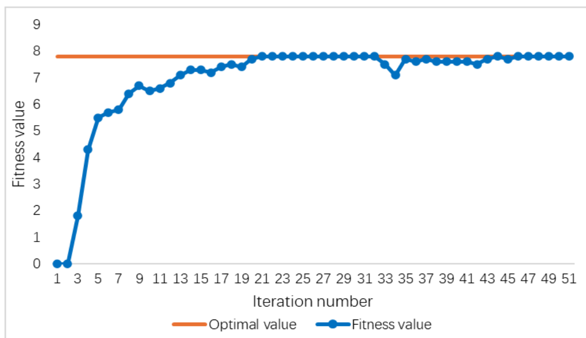

(b) Test image2

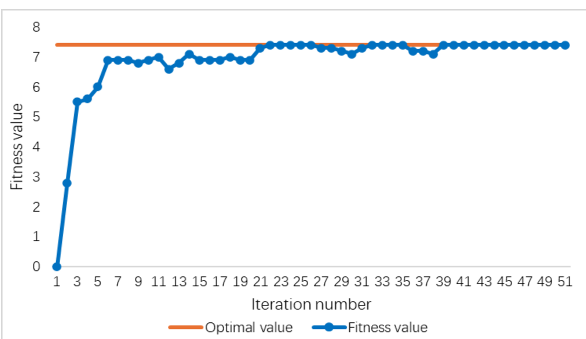

(c) Test image3

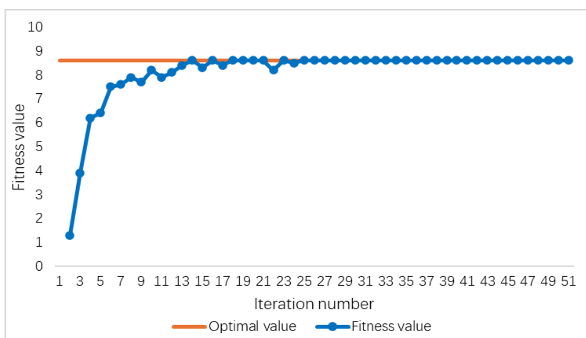

(d) Test image4

Figure 5. Curve of GWO parameter optimization

Figure 6 compares the proposed algorithm with several traditional image processing methods. The first three columns show the original images, local test images, and expert annotations. Subsequent columns display results from morphological differential filtering, homomorphic filtering, illumination normalization, improved Frangi filtering, multi-scale line detection, and the proposed method [12–14].

Results indicate that, compared to morphology, grayscale equalization, differential filtering, and homomorphic filtering, the proposed algorithm better segments thick vessels, preserves details in fuzzy regions, reduces vessel breakage and under-segmentation, and handles noise more effectively. Against improved Frangi and multi-scale line detection methods, it shows stronger recognition of small vessels and terminals, maintains geometric continuity, demonstrates higher robustness, better manages fundus yellow spot interference, and closely matches expert manual results.

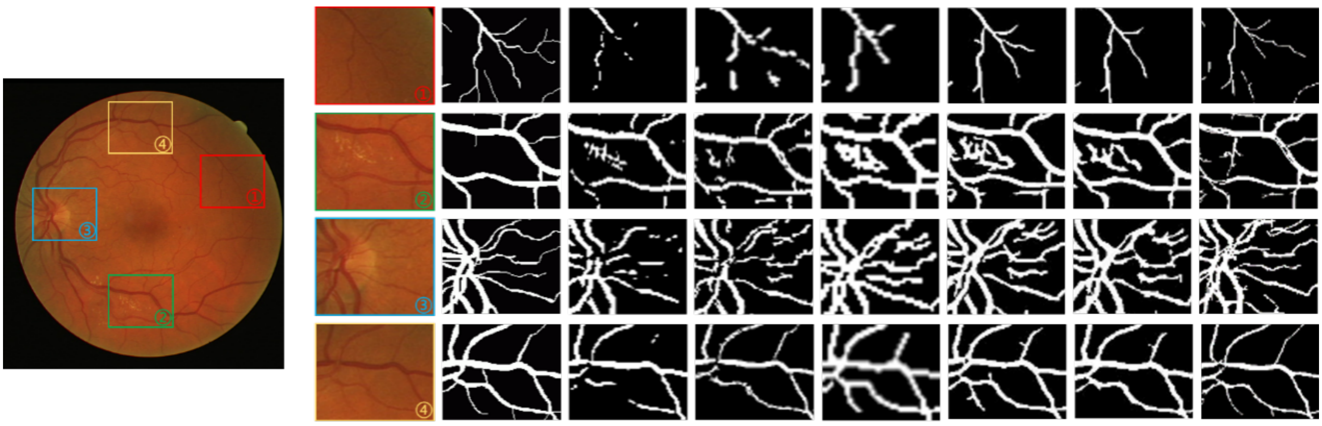

Figure 6. Comparison with the experimental results of classical segmentation algorithm

Figure 7 compares the proposed algorithm with several deep learning models. The first three columns show the test images, local areas, and expert annotations. The following columns display results from U-Net, U-Net with residual network, CNN, Nest U-Net, Dense U-Net, and the proposed method [15–19].

The improved PCNN model performs comparably to U-Net, U-Net + residual network, and CNN, accurately segmenting small and blurred vessels while maintaining vascular continuity. Compared to Nest U-Net and Dense U-Net, it shows fewer false positives, avoids over-segmentation, and achieves higher accuracy in the optic disc area with more complete vessel branches and richer details.

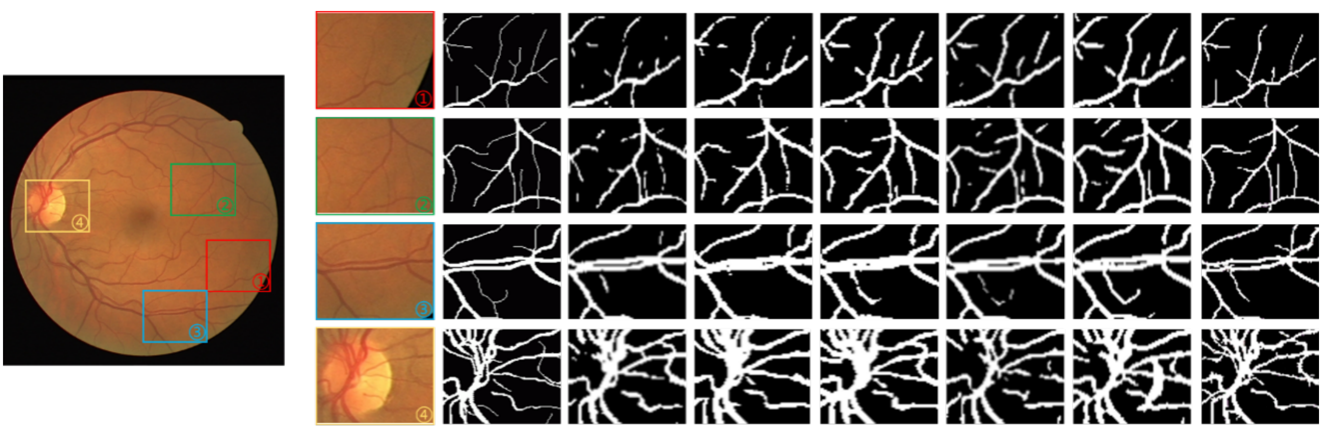

Figure 7. Comparison with the experimental results of deep learning algorithm

6.4. Objective performance analysis

The segmentation experiment was conducted on 20 fundus retinal test images in the fundus image library, the DRIVE dataset. The four performance index values of Sen, Acc, Pre, and Spe of the test results were calculated according to formulas (44) to (47). The average values were 0.799549, 0.962789, 0.889163, and 0.986552, respectively, as shown in **Figure 8**.

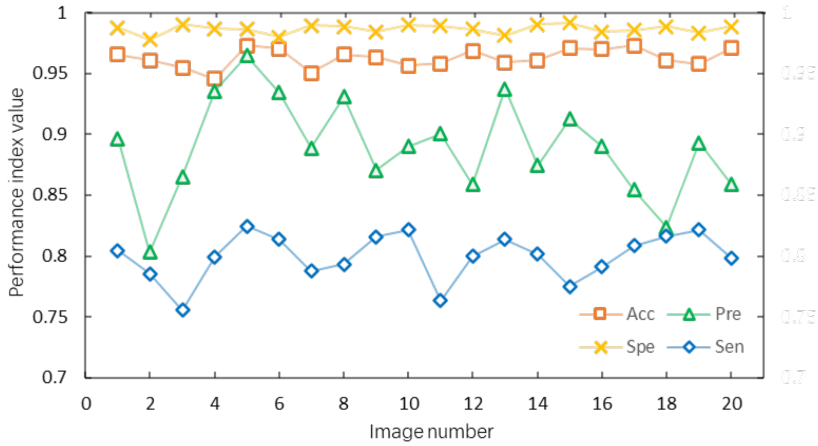

Figure 8. Performance index results for DRIVE

The test results of this paper were compared with several advanced segmentation and machine learning algorithms, as detailed in **Table 1**. Orlando and Adapa used supervised methods [19,20]; Americo, Lian, and Wu employed deep learning [6,16,21], while Ramos-Soto, Neto, and Khan used unsupervised methods [22–24]. The proposed algorithm outperforms classic unsupervised methods in accuracy and specificity, with comparable sensitivity. Without requiring extensive training data, it achieves higher specificity than supervised and deep learning methods, while maintaining similar sensitivity and accuracy.

Table 1. Performance comparison of several typical algorithms

No.	Literature	Method	Year	Sen	Acc	Spe
1	[19]	CRF+SOSVM	2017	0.7897	0.9454	0.9684
2	[20]	Zernike	2020	0.6994	0.9450	0.9811
3	[6]	SWT + FCN	2018	0.8039	0.9821	0.9804
4	[16]	U-Net + Residual Network	2019	0.8278	0.9692	0.9861
5	[5]	U-NET	2020	0.7672	0.9559	0.9834
6	[21]	NFN+	2020	0.7996	0.9582	0.9813
7	[22]	Top-hat + homomorphic filtering+MCET-HHO	2021	0.7578	0.9667	0.9860
8	[23]	GS+MTHT	2017	0.7942	-	0.9631
9	[24]	LD+HT	2018	0.7696	0.9506	0.9651
10	[25]	Matched filtering + fuzzy C clustering	2019	0.761	0.961	0.981
11	[26]	Homomorphic filtering + CLAHE	2020	0.7203	0.9581	0.987
12	[14]	3D filtering	2021	0.8141	0.9399	0.9702
13	[27]	Adaptive contrast enhancement	2021	0.6340	0.9476	0.9803
14	This article	-	-	0.7995	0.9627	0.9865

7. Conclusion

This paper proposes a method for fundus retinal blood vessel segmentation based on improved PCNN and GWO. Based on the traditional PCNN model, by simplifying the traditional PCNN model structure and reducing the model parameter dimension, the neuron connection domain is optimized according to the spatial attributes and intensity information characteristics of the image, the pulse emission ability of the neuron is enhanced, and the image segmentation performance is improved. The GWO algorithm is used to automatically optimize the setting of PCNN model parameters to obtain the optimal parameters for blood vessel segmentation. In addition, a multi-dimensional evaluation standard for fundus retinal blood vessel image segmentation is proposed, and the fitness function of the GWO algorithm is designed based on this, which improves the segmentation performance of PCNN. The test results show that compared with other classic segmentation algorithms, this algorithm can well solve the influence of low illumination, optic disc area, and fovea area on the segmentation results, and the extraction of bifurcated, crossed, closely parallel blood vessels and microvascular terminals is relatively complete; compared with supervised learning models such as U-Net, this algorithm shows excellent vascular connectivity and terminal sensitivity without a large amount of training data. This algorithm still lacks retinal image testing under complex lesions. Therefore, future research directions will focus on the analysis and application of retinal lesion images and other medical images, such as MRI.

Acknowledgments

The authors would like to thank all colleagues and institutions that supported this research, as well as the funding agencies for their generous support.

Funding

The 2019 Guangdong Province General College Youth Innovation Talent Project (2019GKQNCX009)

Disclosure statement

The authors declare no conflict of interest.

References

[1] Wang R, 2015, Method of Retinal Vessel Segmentation based on Particle Swarm Optimization. Computer Engineering and Applications, 51(2): 177–180.

[2] Meng L, Liu J, Cao H, et al., 2019, Retinal Vascular Segmentation based on Frangi filter and Otsu Algorithm. Laser & Optoelectronics Progress, 56(18): 127–133.

[3] Neto LC, Ramalho GLB, Jeova FS, et al., 2017, An Unsupervised Coarse-to-fine Algorithm for Blood Vessel Segmentation in Fundus Images. Expert Systems with Applications, 78: 182–192.

[4] Li Y, Cai Y, Gao X, 2018, Retinal Vessel Segmentation Algorithm based on Hybrid Phase Feature. Journal of Computer Applications, 38(7): 2083–2088.

[5] Cheng Y, Ma M, Zhang L, et al., 2020, Retinal Blood Vessel Segmentation based on Densely Connected U-Net. Mathematical Biosciences and Engineering, 17(4): 3088–3108.

[6] Americo O, Sergio P, Carlos A, et al., 2018, Retinal Vessel Segmentation based on Fully Convolutional Neural Networks. Expert Systems with Applications, 112: 22–242.
[7] Zhang K, Tan Z, Li B, 2018, Automatic Image Segmentation based on Pulse Coupled Neural Network with Particle Swarm Optimization and Comprehensive Evaluation. Optical Precision Engineering, 26(4): 962–970.
[8] Wen C, Wang S, Yu H, et al., 2013, Image Segmentation Method for Maize Diseases based on Pulse Coupled Neural Network with Modified Artificial Bee Algorithm. Transactions of the Chinese Society of Agricultural Engineering (Transactions of the CSAE), 29(13): 142–149.
[9] Qu S, Yang H, 2015, PCNN Infrared Image Segmentation based on Genetic Algorithm Parameter Optimization. High Power Laser and Particle Beams, 27(5): 38–43.
[10] Fan X, Wang J, Shi P, et al., 2021, Pavement Crack Segmentation Algorithm based on Pulse Coupled Neural Network with Brainstorming Optimization. Journal of Southwest Jiao Tong University, 56(3): 572–578.
[11] Mirjalili S, Mirjalili SM, Lewis A, 2014, Grey Wolf Optimizer. Advances in Engineering Software, 69(3): 46–61.
[12] Dash S, Senapati MR, Sahu PK, et al., 2020, Illumination Normalized based Technique for Retinal Blood Vessel Segmentation. International Journal of Imaging Systems and Technology, 31(1): 351–363.
[13] Khawaja A, Khan TM, Naveed K, et al., 2019, An Improved Retinal Vessel Segmentation Framework Using Frangi Filter Coupled with the Probabilistic Patch-based Denoiser. IEEE Access, 7: 164344–164361.
[14] Naveed K, Abdullah F, Madni HA, et al., 2021, Towards Automated Eye Diagnosis: An Improved Retinal Vessel Segmentation Framework Using Ensemble Block Matching 3D Filter. Diagnostics, 11(1): 114.
[15] Ronneberger O, Fischer P, Brox T, 2017, U-Net: Convolutional Networks for Biomedical Image Segmentation. Bildverarbeitung für die Medizin, Cham: Springer Vieweg, 234–241.
[16] Lian S, Li L, Lian G, et al., 2021, A Global and Local Enhanced Residual U-Net for Accurate Retinal Vessel Segmentation. IEEE/ACM Transactions on Computational Biology and Bioinformatics, 18(3): 852–862.
[17] Jiang Z, Zhang H, Wang Y, et al., 2018, Retinal Blood Vessel Segmentation using Fully Convolutional Network with Transfer Learning. Computerized Medical Imaging and Graphics, 68: 1–15.
[18] Wang C, Zhao Z, Yu Y, 2021, Fine Retinal Vessel Segmentation by Combining Nest U-Net and Patch-learning. Soft Computing, 25(1): 5519–5532.
[19] Orlando JI, Prokofyeva E, Blaschko MB, 2017, A Discriminatively Trained Fully Connected Conditional Random Field Model for Blood Vessel Segmentation in Fundus Images. IEEE Transactions on Biomedical Engineering, 64(1): 16–27.
[20] Adapa D, Raj ANJ, Alisetti SN, et al., 2020, A Supervised Blood Vessel Segmentation Technique for Digital Fundus Images Using Zernike Moment-based Features. Plos one, 15(3): e0229831.
[21] Wu Y, Xia Y, Song Y, et al., 2020, NFN+: A Novel Network Followed Network for Retinal Vessel Segmentation. Neural Networks, 126: 153–162.
[22] Ramos-Soto O, Rodriguez-Esparza E, Balderas-Mata SE, et al., 2021, An Efficient Retinal Blood Vessel Segmentation in Eye Fundus Images Using Optimized Top-Hat and Homomorphic filtering. Computer Methods and Programs in Biomedicine, 201: 105949.
[23] Neto LC, Ramalho GLB, Neto JFSR, et al., 2017, An Unsupervised Coarse-to-fine Algorithm for Blood Vessel Segmentation in Fundus Images. Expert Systems with Applications, 78: 182–192.
[24] Khan MAU, Khan TM, Bailey DG, et al., 2019, A Generalized Multi-scale Line-detection Method to Boost Retinal Vessel Segmentation Sensitivity. Pattern Analysis and Applications, 22(3): 1177–1196.
[25] Memari N, Ramli AR, Saripan MIB, et al., 2019, Retinal Blood Vessel Segmentation by Using Matched Filtering

and Fuzzy C-means Clustering with Integrated Level Set Method for Diabetic Retinopathy Assessment. Journal of Medical and Biological Engineering, 39: 713–731.

[26] Dash S, Senapati MR, Sahu PK, et al., 2020, Illumination Normalized based Technique for Retinal Blood Vessel Segmentation. International Journal of Imaging Systems and Technology, 31(1): 351–363.

[27] Dikkala U, Joseph MK, Alagirisamy M, A Comprehensive Analysis of Morphological Process Dependent Retinal Blood Vessel Segmentation. International Conference on Computing, Communication, and Intelligent Systems (ICCCIS), IEEE Press, Piscataway, NJ, 510–516.